The Anti-Inflammatory Activity of *Eucommia ulmoides* Oliv. Bark. Involves NF-κB Suppression and Nrf2-Dependent HO-1 Induction in BV-2 Microglial Cells

Seung-Hwan Kwon, Shi-Xun Ma, Ji-Young Hwang, Yong-Hyun Ko, Ji-Yeon Seo, Bo-Ram Lee, Seok-Yong Lee and Choon-Gon Jang*

Department of Pharmacology, School of Pharmacy, Sungkyunkwan University, Suwon 16419, Republic of Korea

Abstract

In the present study, we investigated the anti-inflammatory properties of *Eucommia ulmoides* Oliv. Bark. (EUE) in lipopolysaccharide (LPS)-stimulated microglial BV-2 cells and found that EUE inhibited LPS-mediated up-regulation of pro-inflammatory response factors. In addition, EUE inhibited the elevated production of pro-inflammatory cytokines, mediators, and reactive oxygen species (ROS) in LPS-stimulated BV-2 microglial cells. Subsequent mechanistic studies revealed that EUE suppressed LPS-induced phosphorylation of mitogen-activated protein kinases (MAPKs), phosphoinositide-3-kinase (PI3K)/Akt, glycogen synthase kinase-3β (GSK-3β), and their downstream transcription factor, nuclear factor-kappa B (NF-κB). EUE also blocked the nuclear translocation of NF-κB and inhibited its binding to DNA. We next demonstrated that EUE induced the nuclear translocation of nuclear factor erythroid 2-related factor 2 (Nrf2) and upregulated heme oxygenase-1 (HO-1) expression. We determined that the significant up-regulation of HO-1 expression by EUE was a consequence of Nrf2 nuclear translocation; furthermore, EUE increased the DNA binding of Nrf2. In contrast, zinc protoporphyrin (ZnPP), a specific HO-1 inhibitor, blocked the ability of EUE to inhibit NO and PGE_2 production, indicating the vital role of HO-1. Overall, our results indicate that EUE inhibits pro-inflammatory responses by modulating MAPKs, PI3K/Akt, and GSK-3β, consequently suppressing NF-κB activation and inducing Nrf2-dependent HO-1 activation.

Key Words: *Eucommia ulmoides* Oliv. Bark., Pro-inflammatory responses, Nuclear factor-kappa B, Nuclear factor erythroid 2-related factor 2, Heme oxygenase-1, BV-2 microglial cells

INTRODUCTION

Microglia are immune cells resident in the central nervous system (CNS) that respond to extracellular stimuli and play a crucial role in the progress of neuro-inflammation (Rock *et al.*, 2004). Chronic neuro-inflammation is a hallmark of neurodegenerative diseases, such as Alzheimer's disease (AD), Parkinson's disease (PD), and stroke (Marchetti and Abbracchio, 2005; Gao and Hong, 2008). In response to extracellular stimuli, microglia can produce and release pro-inflammatory mediators such as nitric oxide (NO), prostaglandin E_2 (PGE_2), reactive oxygen species (ROS), interleukin-1 beta (IL-1β), and tumor necrosis factor-alpha (TNF-α). These mediators help restore CNS homeostasis by clearing pathogens and infected cells. However, prolonged microglial activation can also cause chronic neuro-inflammation and promote neuronal injury due to the increased production of neurotoxic pro-inflammatory mediators, and can eventually lead to neuronal cell death (Boje and Arora, 1992; Block and Hong, 2005; Lull and Block, 2010; Park *et al.*, 2013). Thus, controlling microglial activation may have a therapeutic benefit for many neurodegenerative diseases.

Inflammation is the organized response of an organism to injuries of multiple pathologies. The inflammatory response involves the rapid up-regulation of many genes. Nuclear factor-kappa B (NF-κB) is a critical transcription factor involved in the inflammatory response, and is also known to play an important role in neurodegenerative diseases (O'Neill and Kaltschmidt, 1997). NF-κB is normally bound to inhibitor of nuclear factor kappa B alpha (IκBα) in the cytosol in an inactive form. How-

www.biomolther.org

ever, in response to stress, phosphorylated IκBα is degraded through selective ubiquitination, resulting in NF-κB activation. Activated NF-κB then translocates into the nucleus and binds to the promoter regions of pro-inflammatory molecules, thereby upregulating the expression of multiple target genes (Nomura, 2001). Ultimately, NF-κB induces the expression of many inflammatory mediators, including inducible nitric oxide synthase (iNOS), cyclooxygenase-2 (COX-2), and TNF-α, via the binding of NF-κB to specific promoter regions. Therefore, the modulation of NF-κB activation is a promising strategy for the treatment of many neuropathologies (Baima et al., 2010).

Nuclear factor erythroid 2-related factor 2 (Nrf2) is a redox-sensitive transcription factor that is normally sequestered in the cytoplasm by the regulatory protein Kelch-like ECH-associated protein 1 (Keap1). Under conditions of oxidative or xenobiotic stress, Keap1 undergoes structural modification. Nrf2 is then released from Keap1, translocates to the nucleus, and subsequently binds to a promoter sequence known as the antioxidant response element (ARE). Nuclear accumulation of Nrf2 thus results in the up-regulation of phase II detoxifying anti-oxidant enzymes such as NAD(P)H, quinone oxidore-ductase, heme oxygenase-1 (HO-1), the glutamate-cysteine ligase catalytic subunit, and the glutamate-cysteine ligase modifier subunit (Kensler et al., 2007; Kim et al., 2010). Recent studies have demonstrated that up-regulation of the Nrf2-dependent HO-1 pathway reduces the inflammatory reaction in activated microglia. Moreover, the induction of HO-1 expression in the brain has been shown to be important in neuro-inflammation, neuroprotection, and neuroplasticity. Consequently, Nrf-2 and HO-1 are considered to be important targets for the treatment of neurodegenerative diseases (Bauer and Bauer, 2002; Krönke et al., 2003).

Eucommia ulmoides Oliv. Bark. (EUE) is a traditional tonic medicine used in Korea, China, and Japan. EUE is typically consumed as a tea for the purpose of lowering blood pressure, treating miscarriage, improving liver and kidney tone, and promoting longevity (Kwan et al., 2003; Lee et al., 2005; Luo et al., 2010; Jiang et al., 2011). In addition, EUE has been reported to exert anti-oxidant, anti-inflammatory, anti-tumorigenic, anti-apoptotic, and anti-cancer effects (Yang et al., 2003; Kim et al., 2009; Lin et al., 2011; Kim et al., 2012; Liu et al., 2012). In our previous studies, we showed that EUE exhibits anti-oxidative stress and anti-acetylcholinesterase activities in the brain and neuronal cells, in addition to providing neuroprotective effects against the amyloid beta peptide25-35 and hydrogen peroxide (H₂O₂) (Kwon et al., 2011; Kwon et al., 2012). EUE is thus a candidate agent for the treatment of neurological diseases, including AD. These reports indicate the importance of determining the relationship between EUE and neurodegenerative diseases; however, the actions and mechanisms of EUE in neuro-inflammation-related disorders have been poorly elucidated. Moreover, no report to date has investigated the molecular mechanisms of the anti-inflammatory activities of EUE in LPS-stimulated BV-2 microglial cells.

In the present study, we investigated whether EUE exerts anti-inflammatory effects. Specifically, we studied the mechanisms of action of EUE on LPS-stimulated pro-inflammatory responses in BV-2 microglial cells. We investigated whether EUE inhibits NF-κB activation and whether EUE activates Nrf2-dependent signaling, which leads to HO-1 up-regulation in an event that is downstream of ARE-responsive proteins. We also determined whether EUE-induced activation of Nrf2-

dependent HO-1 signaling is the major cellular mechanism mediating the anti-inflammatory effects of EUE.

MATERIALS AND METHODS

Materials

2,7'-Dichlorofluorescin diacetate (DCFH-DA), dimethyl sulfoxide (DMSO), Hoechst 33258, 3-(4,5-dimethyl thiazol-2-yl)-2,5-diphenyl tetrazolium bromide (MTT), lipopolysaccharide (LPS, Escherichia coli, 026:B6), poly-D-lysine, and anti-β-actin antibodies were purchased from Sigma Chemical Co. (St. Louis, MO, USA). Zinc protoporphyrin (ZnPP) was purchased from Tocris Cookson (Bristol, UK). Dulbecco's modified Eagle's medium (DMEM) was obtained from HyClone (Logan, UT, USA). Fetal bovine serum (FBS), 0.25% trypsin-EDTA, and penicillin/streptomycin were obtained from GIB-CO-BRL (Grand Island, NY, USA). Rabbit anti-phospho-Akt (Ser473), rabbit anti-phospho-ERK1/2 (Thr202/Tyr204), rabbit anti-ERK 1/2 (Thr202/Tyr204), rabbit anti-phospho-GSK-3α/β (Ser21/9), rabbit anti-glycogen synthase kinase-3 α/β (GSK-3α/β) (D75D3), rabbit anti-phospho-JNK (Thr183/Tyr185), rabbit anti-JNK (Thr183/Tyr185), rabbit anti-lamin B1, rabbit anti-NF-κB p65, and anti-rabbit horseradish peroxidase-linked IgG antibodies were purchased from Cell Signaling (Boston, MA, USA). Rabbit anti-COX-2, rabbit anti-HO-1, rabbit anti-phospho-IκBα, rabbit anti-IκBα, rabbit anti-phospho-p38 MAPK (Thr180/Tyr182), and rabbit anti-p38 MAPK (Thr180/Tyr182) antibodies were purchased from Epitomics Inc (Abcam, Burlingame, CA, USA). Rabbit anti-Akt (Ser473), rabbit anti-Nrf2, and rabbit anti-iNOS antibodies were obtained from Santa Cruz Biotechnology, Inc. (Santa Cruz, CA, USA). Alexa Fluor® 488-conjugated goat anti-rabbit IgG antibodies, Texas Red®-conjugated goat anti-rabbit IgG antibodies, and Lipofectamine® 2000 transfection reagent were purchased from Invitrogen (Molecular Probes, Eugene, OR, USA). PCR primers were synthesized by Cosmogenetech (Seoul, Republic of Korea). All other chemicals were of analytical grade and were purchased from Sigma Chemical.

Preparation of EUE extract

The dried stem bark of Eucommia ulmoides Oliv. was purchased from the Kyung-Dong Oriental Medicine Market (Seoul, Republic of Korea). The stem bark of EU had been collected in Andong, Republic of Korea in June 2008 and was identified by Professor Sun Yeou Kim (College of Pharmacy, Gachon University, Incheon, Republic of Korea). A voucher specimen (KSYHP-EC-002-ET) was deposited at the herbarium of the Graduate School of East-West Medical Science, Kyung Hee University. The dried EU bark was cut into small pieces and extracted in hot water (70°C) three times using a reflux apparatus with a cooling system (40°C) for 1 h, and the resultant aqueous extract was passed through filter paper (Whatman, No. 2, Florham Park, NJ, USA). The supernatants were concentrated under reduced pressure with a vacuum rotary evaporator (EYELA, N-1000, Tokyo, Japan) and then lyophilized. Finally, the supernatant (100 g) was extracted with ethyl acetate three times for 1 h in an ultrasonic apparatus. The supernatant was evaporated and spray-dried, thus yielding 5 g of EUE that was stored at -20°C until use.

Cell culture and treatment

BV-2 microglial cells were grown in DMEM supplemented with 10% heat-inactivated FBS (v/v) and 0.1% penicillin/streptomycin (v/v) in a humidified atmosphere of 5% CO_2 and 95% air at 37°C. LPS was prepared immediately before use as a 10 μg/ml stock and diluted in PBS to the indicated final concentration, while EUE was dissolved in DMSO. All stock solutions were added directly to the culture medium. Control cells were treated with DMSO only. The final concentration of solvent was always <0.1% (v/v). No significant cytotoxicity was observed in any of the experiments (data not shown). In all experiments, cells were treated with the indicated concentrations of EUE in the presence or absence of LPS (100 ng/ml) in serum-free DMEM.

Cell viability assay

Cell viability was measured based on the formation of formazan, a blue product resulting from the metabolism of a colorless substrate (MTT) by mitochondrial dehydrogenases, which are active only in live cells. BV-2 microglial cells ($2.5×10^5$ cells/well in 24-well plates) were incubated at 37°C with LPS for 24 h with or without EUE pretreatment and then treated with an MTT solution (5 mg/ml) for 2 h. The dark blue formazan crystals formed in intact cells were dissolved in DMSO and the resultant absorbances were measured at 540 nm with a microplate reader (SpectraMax 250, Molecular Device, Sunnyvale, CA, USA). Results are expressed as the percentage of metabolized MTT relative to that of control cells as determined by absorbance measurements.

Determination of NO production

NO release into culture supernatants was measured by the Griess reaction. In brief, BV-2 microglial cells ($2.5×10^5$ cells/well in 24-well plates) were incubated at 37°C with LPS for 24 h with or without EUE pretreatment. 100 μl of culture supernatant from each sample was then mixed with an equal volume of Griess reagent [0.1% N-(1-naphthyl)-ethylenediamine dihydrochloride and 1% sulfanilamide in 5% phosphoric acid] in 96-well plates for 10 min at room temperature in the dark. Nitrite concentrations were determined by reference to standard solutions of sodium nitrite prepared in cell culture medium. The absorbances at 540 nm were determined using a microplate reader.

Enzyme-linked immunosorbent assay (ELISA)

The levels of PGE_2, TNF-α, and IL-1β were determined using specific ELISA kits (PGE_2 kit, Cayman Chemical, Ann Arbor, MI, USA; TNF-α and IL-1β kits, KOMA Biotech, Seoul, Korea) as per the manufacturers' instructions.

Measurement of intracellular ROS accumulation

BV-2 microglial cells ($1×10^6$ cells/well) were seeded on 6-well plates or poly-D-lysine coated slides and cultured overnight. The levels of intracellular ROS were measured using DCFH-DA. After pretreatment with or without EUE for 30 min, the cells were incubated with LPS for 24 h. The cells were rinsed with PBS and treated with 10 μM DCFH-DA (for 30 min) and 5 μg/ml Hoechst 33258 (for 5 min) at 37°C, washed twice with PBS, and the resultant fluorescence was measured at 530 nm with a microplate reader (SpectraMax M2, Molecular Device, Sunnyvale, CA, USA) with excitation at 488 nm. DCFH-DA fluorescence images were captured with a fluorescence microscope (20x).

RNA isolation and reverse transcription-polymerase chain reaction (RT-PCR)

BV-2 microglial cells ($1×10^6$ cells/well in 6-well plates) were incubated at 37°C with LPS, with or without pretreatment with EUE. Total RNA was isolated using Trizol® reagent (Invitrogen). Reverse transcription was carried out with a Superscript®-III kit (Invitrogen) using 5 μg total RNA and oligo dT according to the manufacturer's instructions. Specific primer sequences were as follows: iNOS (forward, 5'-CTGCAG-CACTTGGATCAGGAACCTG-3' and reverse, 5'-GGGAG-TAGCCTGTGTGCACCTGGAA-3'), COX-2 (forward, 5'-TTGA-AGACCAGGAGTACAGC-3' and reverse, 5'-GGTACAGTTC-CATGACATCG-3'), TNF-α (forward, 5'-CGTCAGCCGATTT-GCTATCT-3' and reverse, 5'-CGGACTCCGCAAAGTCTA-AG-3'), IL-1β (forward,5'-GCCCATCCTCTGTGACTCAT-3'and reverse, 5'-AGGCCACAGGTATTTTGTCG-3'), HO-1 (forward, 5'-CAAGCCGAGAATGCTGAGTTCATG-3' and reverse, 5'-GCAAGGGATGATTTCCTGCCAG-3'), and β-actin (forward, 5'-AGCCATGTACGTAGCCATCC-3' and reverse, 5'-GCTGT-GGTGGTGAAGCTGTA-3'). PCR amplification of the resulting cDNA template was conducted for 25 (iNOS, COX-2, HO-1, and β-actin) or 30 (TNF-α and IL-1β) cycles. Briefly, after an initial denaturation step at 95°C for 2 min, thermal cycling was initiated. Each cycle consisted of denaturation at 95°C for 1 min, annealing at 65°C (iNOS), 55°C (COX-2), 57°C (TNF-α and IL-1β), 60°C (HO-1), or 58°C (β-actin) for 1 min, extension at 72°C for 1 min, and a final extension at 72°C for 5 min. PCR products were analyzed by staining with ethidium bromide after electrophoresis for 30 min at 100 V on 1.5% agarose gels in Tris borate/EDTA buffer (890 mM Tris base, 890 mM boric acid, 20 mM EDTA, pH 8.3). Amplicons were visualized on a UV transilluminator and their intensities quantified by densitometric analysis using ImageJ software (NIH Image, public domain, USA).

Preparation of nuclear and cytosolic fractions of cell lysates

BV-2 microglial cells were seeded at $5×10^6$ cells/well in 100 mm^2 cell culture dishes. After pretreatment with EUE, the cells were incubated either with or without LPS. To evaluate the nuclear translocation of NF-κB p65, nuclear and cytosolic fractions were prepared using NE-PER nuclear and cytoplasmic extraction reagents for cultured cells (Pierce, Rockford, IL, USA) according to the manufacturer's instructions. The levels of NF-κB p65 and Nrf2 were determined by Western blot analysis and electrophoretic mobility shift assays (EMSA) were performed as described below.

Western blot analysis

BV-2 microglial cells were seeded at $1×10^6$ cells/well in 6-well plates. After pretreatment with EUE, the cells were incubated either with or without LPS. Cells were then washed with ice-cold PBS and harvested by scraping with 100 μl ice-cold T-PER tissue protein extraction buffer (Thermo Scientific, Rockford, IL, USA) containing a protease and phosphatase inhibitor cocktail (Roche Diagnostics GmbH, Mannheim, Germany). Lysates were incubated on ice for 30 min. After centrifugation at 10,000×*g* for 15 min, the supernatants were removed and stored at -70°C. The protein concentrations were determined using a protein assay kit (Thermo Scientific). Proteins were
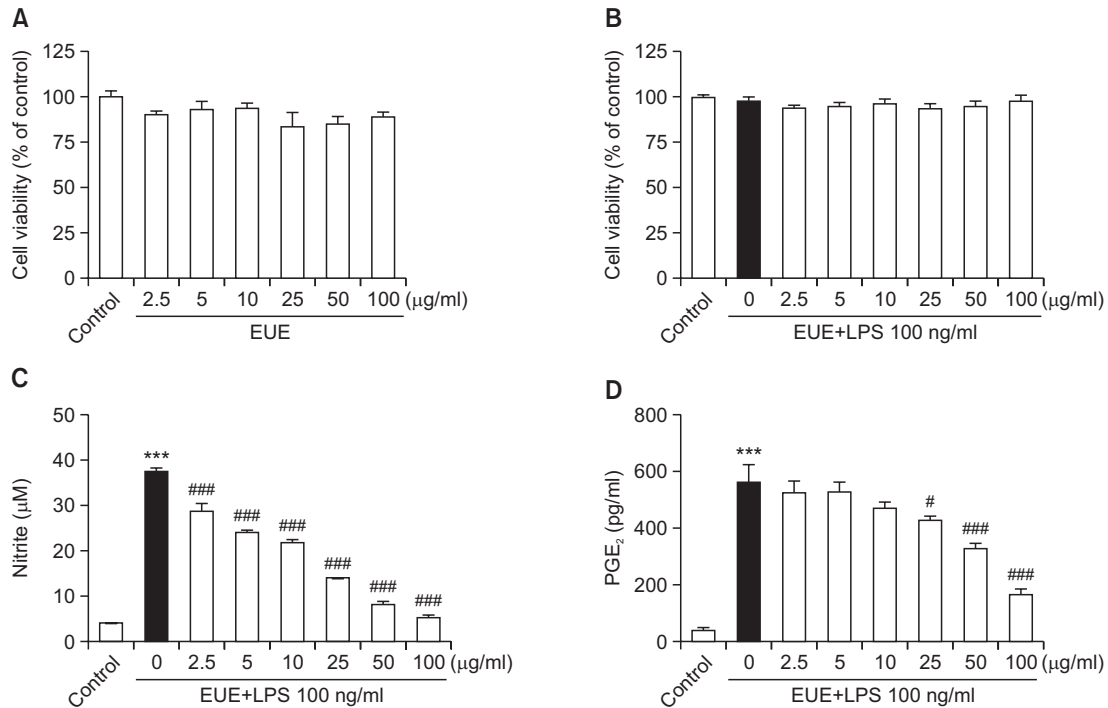
Fig. 1. Effects of EUE on the viability of BV-2 microglial cells (A). Cells were treated with the indicated concentrations of EUE for 24 h. Effects of EUE on LPS-induced cell death in BV-2 microglial cells (B). Cell viability was assessed by the MTT assay and is expressed as a percentage of the corresponding value of control cells. Cells were pretreated with the indicated concentrations of EUE for 30 min and then stimulated with 100 ng/ml LPS for 24 h. Effects of EUE on LPS-induced production of NO (C) and PGE2 (D) in BV-2 microglial cells. Cells were pretreated with the indicated concentrations of EUE for 30 min and then stimulated with 100 ng/ml LPS for 24 h. The concentrations of nitrite in the culture medium were then determined by the Griess reagent. The PGE2 concentrations in the culture medium were measured using a commercial ELISA kit. Data are presented as means ± S.E.M. (n=6). ***$p<0.001$ compared with the control group. #$p<0.05$ and ###$p<0.001$ compared with the LPS-treated group.

separated on 8-12% SDS-polyacrylamide gels and then transferred to polyvinylidene difluoride membranes (Pall Corporation, Pensacola, FL, USA). Nonspecific binding sites were blocked with 5% skim milk in TBST buffer [0.5 mM Tris-HCl (pH 7.5), 150 mM NaCl, and 0.1% Tween-20] for 1 h at room temperature. The membranes were subsequently incubated with primary antibodies overnight at 4°C [antibodies against HO-1, iNOS, phospho-JNK (Thr183/Tyr185), JNK, phospho-ERK1/2 (Thr202/Tyr204), ERK 1/2 (Thr202/Tyr204), phospho-Akt (Ser473), Akt (Ser473), phospho-GSK-3α/β (Ser21/9), GSK-3α/β (D75D3), NF-κB p65, Nrf2, and lamin were used at a dilution of 1:1,000; against β-actin at a dilution of 1:20,000; against COX-2 at a dilution of 1:500; and against IκBα and phospho-IκBα at a dilution of 1:10,000]. After three washes with TBST, the membranes were incubated with horseradish peroxidase-conjugated secondary antibodies (1:5,000) in TBST with 5% nonfat milk for 1 h at room temperature. The membranes were then washed three more times in TBST. Immunoreactive bands were visualized by enhanced chemiluminescence. Specifically, the membranes were immersed for 5 min in a 1:1 ratio of ECL reagents A and B (Animal Genetics, Suwon, Republic of Korea) and then exposed to photographic film. Band intensities were quantified by densitometric analysis using ImageJ software.

Transient transfection and dual-luciferase assay

NF-κB and ARE reporter constructs were purchased from SABiosiences (Qiagen, Valencia, CA, USA). In brief, BV-2 microglial cells were plated in 24-well plates at a density of 2.5×10^5 cells/well and grown overnight. Cells were cotransfected with 5 μg/ml of an NF-κB reporter plasmid, an ARE reporter plasmid, or a negative control plasmid along with an internal control plasmid to measure transfection efficiency. Transfections were performed for 6 h using lipofectamine. After transfection, cells were cultured in medium with 10% FBS for 24 h. Twenty-four hours after transfection, the cells were incubated with EUE and then treated either with or without LPS. Luciferase activity was assayed using a dual-luciferase assay kit (Promega, Madison, WI, USA) according to the manufacturer's instructions. Luminescence was measured using a single tube luminometer (FB12, Berthold Detection Systems GmbH, Pforzheim, Germany).

Electrophoretic mobility shift assay (EMSA)

Nuclear extracts were prepared using the NE-PER nuclear and cytoplasmic extraction reagents as described above. Synthetic complementary NF-κB-binding (5'-AGTTGAGGGGACTTTCCCAGGC-3') and Nrf2-binding (5'-GCTCTTCCGGTGCTCTTCCGGT-3') oligonucleotides (Affimetrix Inc., CA, USA) were 5'-biotinylated using a biotin 5'-end DNA labeling EMSA kit (Affimetrix Inc.) according to the manufacturer's protocol. The binding reactions contained 10 μg of nuclear extract proteins, binding buffer, 1 μg of poly d(I-C), and 10 ng of biotin-labeled DNA. The reactions were incubated for 5 min at
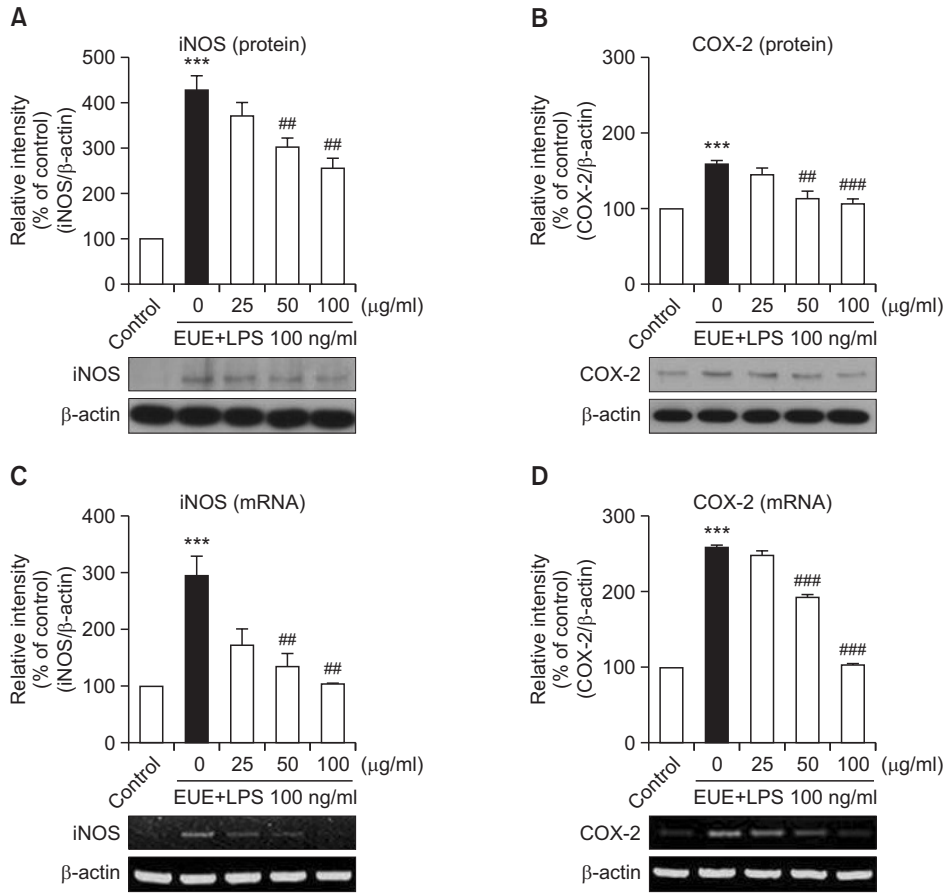
Fig. 2. Effects of EUE on LPS-mediated upregulation of the protein and mRNA levels of iNOS (A and C) and COX-2 (B and D) in BV-2 microglial cells. Cells were pretreated with the indicated concentrations of EUE for 30 min and then stimulated with 100 ng/ml LPS for 24 h (A and B). The levels of iNOS, COX-2, and β-actin were determined by Western blot analysis. Cells were pretreated with the indicated concentrations of EUE for 30 min and then stimulated with 100 ng/ml LPS for 6 h (C and D). The mRNA expression levels of iNOS, COX-2, and β-actin were determined by RT-PCR. Densitometric results are presented as means ± S.E.M. (n=3). ***p<0.001 compared with the control group. ##*p*<0.01 and ###*p*<0.001 compared with the LPS-treated group.

room temperature in a final volume of 10 μl. The protein-DNA complexes were separated from the DNA probes by electrophoresis on a native 6% polyacrylamide gel that had been pre-electrophoresed for 1 h in 0.5x Tris borate/EDTA buffer (50 mM Tris base, 18 mM boric acid, 500 mM EDTA, pH 8.3). Complexes were then transferred to a positively charged nylon membrane (Pall Corporation, Pensacola, FL, USA) in 0.5x Tris borate/EDTA buffer at 300 mA for 30 min, after which the DNA was hybridized to the nylon membrane in a drying oven at 80°C for 1 h. Horseradish peroxidase-conjugated streptavidin was used according to the manufacturer's instructions to detect the transferred DNA.

Immunocytochemistry

BV-2 microglial cells (5×10⁵ cells/well) were seeded on poly-D-lysine coated culture slides and incubated for 24 h. After pretreatment with EUE, the cells were incubated either with or without LPS. Cells were then washed with PBS and fixed with 4% paraformaldehyde for 15 min. After washing, cells were permeabilized with 0.1% Triton X-100 in PBS for 10 min. Cells were blocked in 5% BSA/PBS for 1 h and then incubated overnight with anti-NF-κB p65 and anti-Nrf2 antibodies (1:250

each). Cells were then washed with PBS and incubated for 1 h with Texas Red®-conjugated goat anti-rabbit IgG antibodies (1:250 for NF-κB p65) or Alexa Fluor® 488-conjugated goat anti-rabbit IgG antibodies (1:250 for Nrf2) and Hoechst 33258 (5 μg/ml) for 5 min. Cells were washed in PBS and mounted on glass slides in Permafluor aqueous mounting medium. All procedures were performed at room temperature. Cells were observed under a fluorescence microscope (100x). The results shown are representative of three independent experiments.

Statistics

Data were analyzed with Prism 5.0 software (GraphPad Software, Inc., San Diego, CA, USA) and are expressed as means ± S.E.M. Statistical analyses were performed using one-way analysis of variance (ANOVA) followed by the Newman-Keuls test. Statistical significance was set at *p*<0.05.

RESULTS

Effects of EUE on the viability of BV-2 microglial cells

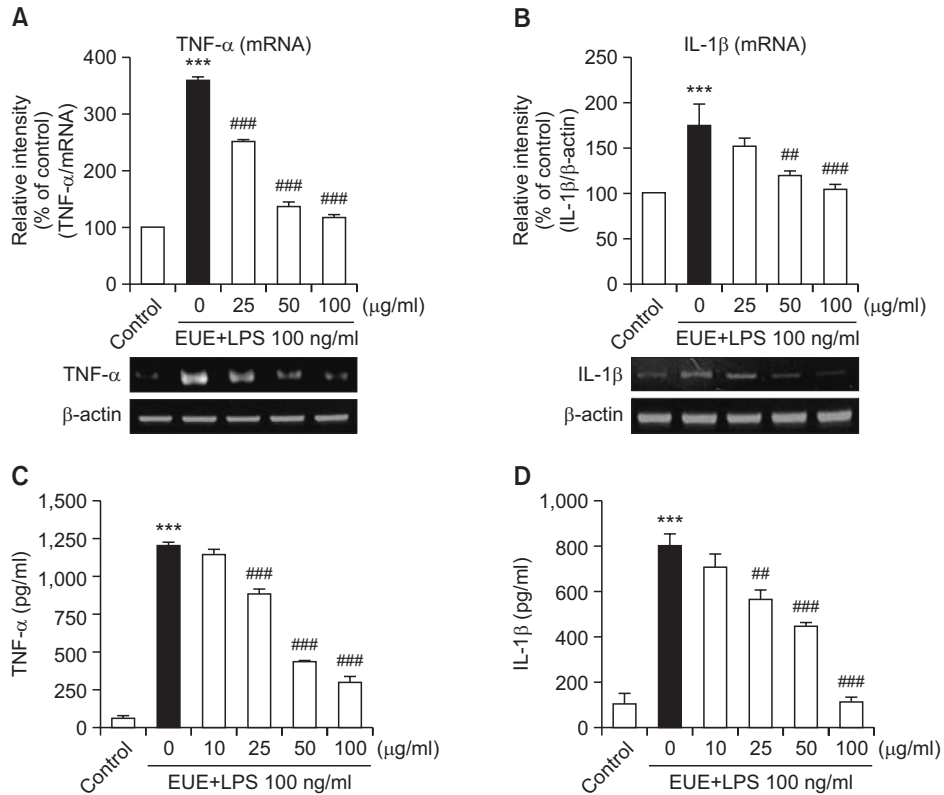To exclude the possibility that the decreases in NO and cy-

Fig. 3. Effects of EUE on LPS-mediated production of TNF-α (A and C) and IL-1β (B and D) in BV- 2 microglial cells. Cells were pretreated with the indicated concentrations of EUE for 30 min and then stimulated with 100 ng/ml LPS for 6 h. The mRNA expression levels of TNF-α, IL-1β, and β-actin were evaluated by RT-PCR. Results are presented as means ± S.E.M. (n=3). Cells were pretreated with the indicated concentrations of EUE for 30 min and then stimulated with 100 ng/ml LPS for 24 h. The concentrations of TNF-α and IL-1β in the culture medium were measured using commercial ELISA kits. Data are presented as means ± S.E.M. (n=6). ***$p<0.001$ compared with the control group. ##$p<0.01$ and ###$p<0.001$ compared with the LPS-treated group.

tokine levels were simply due to cell death, the MTT assay was used to assess the cytotoxicity of EUE in BV-2 microglial cells in the absence or presence of LPS. EUE was not cytotoxic at any of the concentrations (2.5, 5, 10, 25, 50, and 100 μg/ml) used in this study (Fig. 1A, 1B). Thus, these concentrations of EUE were used in subsequent experiments.

Effects of EUE on LPS-induced production of NO and PGE$_2$ in BV-2 microglial cells

We initially evaluated the effects of EUE on NO and PGE$_2$ production in LPS-stimulated BV-2 microglial cells. NO production was assessed by measuring the amount of nitrite released into the culture medium using the Griess reagent. Treatment with LPS significantly increased NO and PGE$_2$ production by 37.63 ± 0.51 μM and 564.60 ± 59.07 pg/ml more than the control values, respectively (Fig. 1C, 1D, $p<0.001$). However, this increased production of NO was significantly inhibited by 2.5, 5, and 10 μg/ml EUE to 28.60 ± 1.83 μM, 24.03 ± 0.46 μM, and 21.87 ± 0.51 μM greater than the control values ($p<0.001$). With 25 μg/ml EUE, the levels of NO and PGE$_2$ production were significantly reduced to 13.83 ± 0.06 μM and 428.00 ± 13.59 pg/ml greater than the control values, respectively ($p<0.05$ and $p<0.001$). Pretreatment with 50 μg/ml EUE also inhibited NO and PGE$_2$ production to 8.20 ± 0.06 μM and 328.50 ± 17.94 pg/ml greater than the control values, respectively ($p<0.001$). In addition, pretreatment with

100 μg/ml EUE dramatically inhibited NO and PGE$_2$ production to 5.33 ± 0.76 μM and 164.00 ± 24.91 pg/ml greater than the control values, respectively ($p<0.001$).

Effects of EUE on LPS-induced up-regulation of iNOS and COX-2 expression at the protein and mRNA levels in BV-2 microglial cells

Since EUE inhibited the production of NO and PGE$_2$, we next examined the relationship between the concentration of EUE and the expression of iNOS and COX-2. Western blot analysis showed that LPS treatment significantly increased the protein levels of iNOS and COX-2 to 430.60 ± 32.22% and 160.50 ± 3.80% of the control values, respectively (Fig. 2A, 2B, $p<0.001$). However, pretreatment with 50 μg/ml EUE significantly attenuated these increases in the protein levels of iNOS and COX-2 to 303.80 ± 20.23% and 113.00 ± 9.72% of the control values, respectively ($p<0.01$). Moreover, pretreatment with 100 μg/ml EUE further decreased the upregulation of iNOS and COX-2 protein levels to 258.30 ± 19.74% and 106.00 ± 7.82% of the control values, respectively ($p<0.001$).

Treatment with LPS also significantly increased the mRNA expression levels of iNOS and COX-2 to 296.00 ± 34.47% and 258.20 ± 4.01% of the control values, respectively (Fig. 2C, 2D, $p<0.001$). However, this induction of iNOS and COX-2 mRNA expression was significantly inhibited by 50 μg/ml EUE to 136.20 ± 23.23% and 192.80 ± 3.09% of the control values,
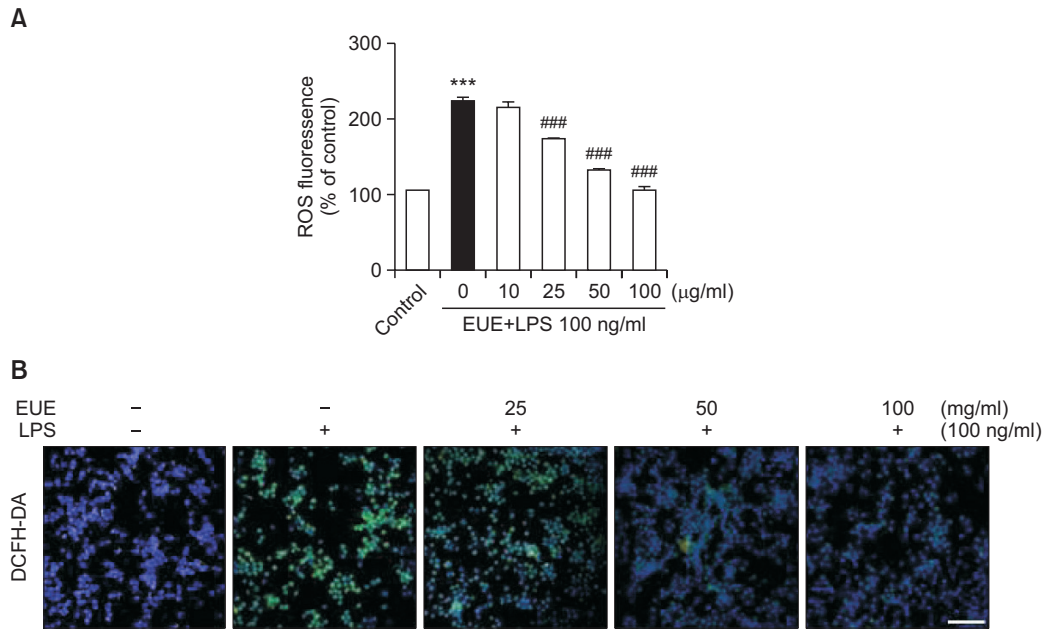
Fig. 4. Effects of EUE on LPS-induced ROS accumulation in BV-2 microglial cells. (A) Cells were pretreated with the indicated concentrations of EUE for 30 min and then stimulated with 100 ng/ml LPS for 24 h. Intracellular ROS accumulation was assayed using DCFH-DA fluorescent dye. Data are presented as means ± S.E.M. (n=6). Nuclei were counterstained with Hoechst 33258, and representative pictures were taken with a fluorescence microscope (B, 20x magnification). The images shown are representative of three experiments. ***$p<0.001$ compared with the control group. ###$p<0.001$ compared with the LPS-treated group. Scale bar: 200 μm.

respectively ($p<0.01$ and $p<0.001$). In addition, pretreatment with 100 μg/ml EUE significantly inhibited this upregulation of iNOS and COX-2 mRNA expression to 104.80 ± 1.02% and 104.10 ± 1.94% of the control values, respectively ($p<0.01$ and $p<0.001$).

Effects of EUE on LPS-induced TNF-α and IL-1β production in BV-2 microglial cells

We next investigated whether EUE inhibits LPS-induced production of TNF-α and IL-1β by RT-PCR and ELISA. Treatment with LPS significantly increased the mRNA levels of these pro-inflammatory cytokines to 361.70 ± 5.59% and 174.40 ± 23.46% of the control values, respectively (Fig. 3A, 3B, $p<0.001$). However, this upregulation of TNF-α mRNA expression was significantly suppressed by 25 μg/ml EUE to 251.70 ± 3.66% of the control value ($p<0.001$). Pretreatment with 50 μg/ml EUE also significantly attenuated the upregulation of TNF-α and IL-1β mRNA expression to 138.20% ± 5.04% and 119.40 ± 5.35% of the control values, respectively ($p<0.01$ and $p<0.001$). In addition, pretreatment with 100 μg/ml EUE markedly inhibited the upregulation of TNF-α and IL-1β mRNA expression to 117.40 ± 5.32% and 104.10 ± 6.28% of the control values, respectively ($p<0.001$).

As a complementary approach, we also performed ELISAs to determine whether EUE inhibits the release of these cytokines *in vitro*. Treatment with LPS significantly increased the levels of secreted TNF-α and IL-1β to 1,210.00 ± 18.94 pg/ml and 803.20 ± 49.88 pg/ml, respectively (Fig. 3C, 3D, $p<0.001$). However, this increased secretion of TNF-α and IL-1β was significantly blocked by pretreatment with 25 μg/ml EUE to 889.30 ± 30.41 pg/ml and 568.20 ± 36.84 pg/ml, respectively ($p<0.01$ and $p<0.001$). Pretreatment with 50 μg/ml

EUE also significantly decreased the levels of secreted TNF-α and IL-1β to 441.10 ± 9.02 pg/ml and 443.20 ± 21.06 pg/ml, respectively ($p<0.001$). In addition, pretreatment with 100 μg/ml EUE markedly inhibited the levels of secreted TNF-α and IL-1β to 301.20 ± 34.66 pg/ml and 108.90 ± 20.98 pg/ml, respectively ($p<0.001$).

Effects of EUE on LPS-induced ROS accumulation in BV-2 microglial cells

We next examined the effect of EUE on the production of ROS, which are known to be early signaling inducers in microglial inflammation that contribute to neuronal cell death and neurodegeneration. Intracellular ROS formation was investigated with DCFH-DA, a fluorescent ROS-sensitive probe. Treatment with LPS significantly increased intracellular ROS production to 222.70 ± 3.19% of the control value (Fig. 4A, $p<0.001$), whereas pretreatment with 25, 50, and 100 μg/ml EUE significantly inhibited these increases in intracellular ROS accumulation to 172.10 ± 1.40%, 131.00 ± 3.65%, and 104.30 ± 4.88% of the control value, respectively ($p<0.001$). To further investigate the effect of EUE on LPS-induced intracellular ROS accumulation, we analyzed the localization of ROS using the DCFH-DA probe. Microphotographs of DCFH-DA staining revealed excessive intracellular ROS accumulation following LPS stimulation (Fig. 4B). Pretreatment with EUE clearly inhibited this staining, indicating a reduction in intracellular ROS accumulation.

Effects of EUE on LPS-induced phosphorylation of JNK, ERK 1/2, p38 MAPKs, PI3K/Akt, and GSK-3α/β in BV-2 microglial cells

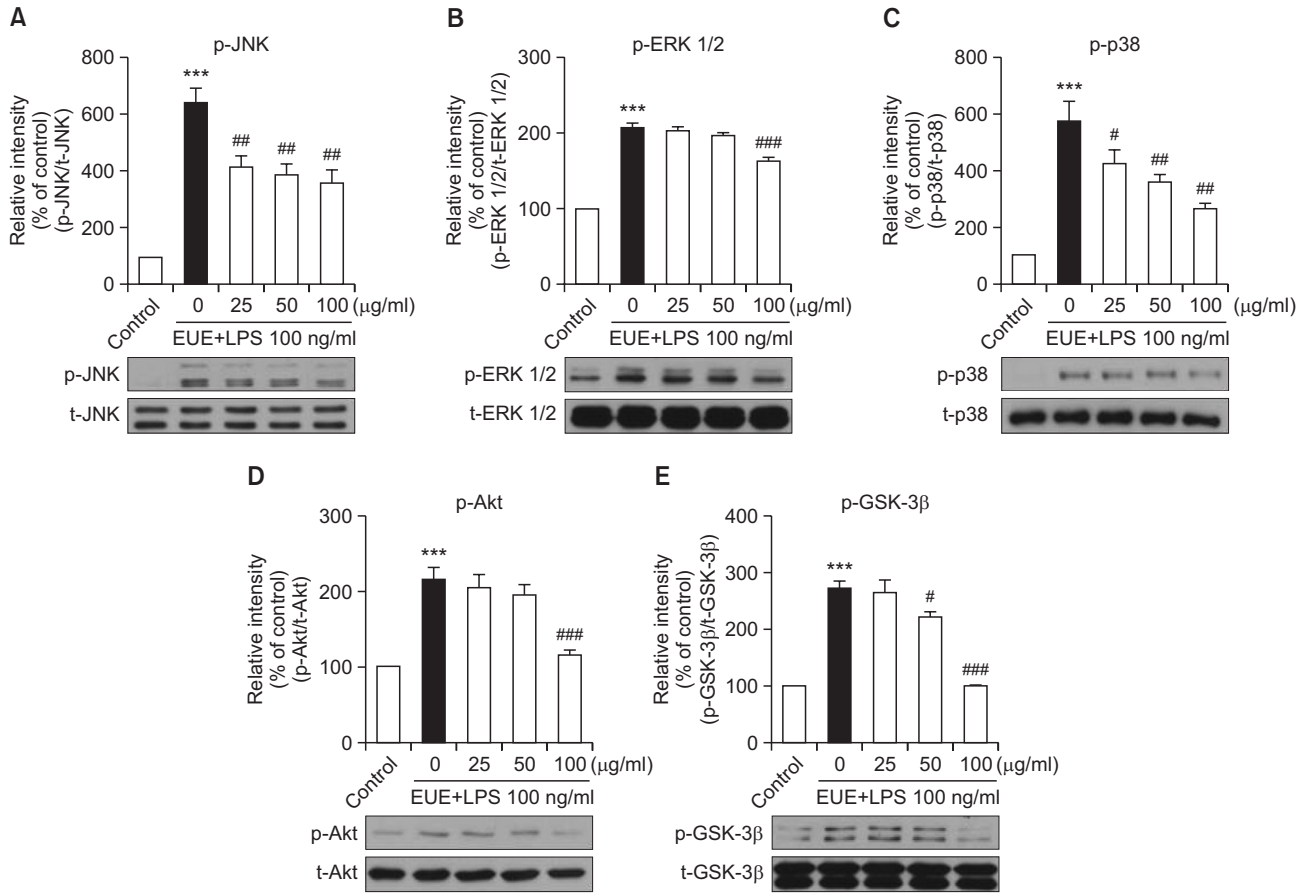To evaluate the effects of EUE on the upstream signaling

Fig. 5. Effects of EUE on LPS-induced phosphorylation of JNK (A), ERK 1/2 (B), p38 MAPKs (C), PI3K/Akt (D), and GSK-3α/β (E) in BV-2 microglial cells. Cells were pretreated with the indicated concentrations of EUE for 30 min and then stimulated with 100 ng/ml LPS for 1 h. The expression levels of JNK, ERK 1/2, p38 MAPKs, PI3K/Akt, and GSK-3α/β were evaluated by Western blot analysis. Densitometric results are presented as means ± S.E.M. (n=3). ***$p < 0.001$ compared with the control group. #$p < 0.05$; ##$p < 0.01$; and ###$p < 0.001$ compared with the LPS-treated group.

pathways associated with NF-κB translocation, we examined changes in the activation of intracellular signaling proteins such as JNK, ERK 1/2, p38 MAPKs, PI3K/Akt, and GSK-3β in BV-2 microglial cells. As shown in Fig. 5, treatment with LPS rapidly increased the phosphorylation of JNK, p38 MAPKs, ERK 1/2, PI3K/Akt, and GSK-3β to 649.90 ± 47.70%, 207.50 ± 5.44%, 575.70 ± 69.37%, 215.40 ± 14.56%, and 274.90 ± 10.35% of the control values, respectively (Fig. 5, $p < 0.001$). However, the increased phosphorylation of JNK and p38 MAPK was significantly inhibited by 25 μg/ml EUE to 418.00 ± 38.50% and 423.90 ± 47.77% of the control values, respectively ($p < 0.05$ and $p < 0.01$). Pretreatment with 50 μg/ml EUE also significantly suppressed the increased phosphorylation of JNK, p38 MAPKs, and GSK-3β to 393.00 ± 35.04%, 359.70 ± 25.49%, and 222.50 ± 8.05% of the control values, respectively ($p < 0.05$ and $p < 0.01$). Moreover, pretreatment with 100 μg/ml EUE dramatically suppressed the increased phosphorylation of JNK, ERK 1/2, p38 MAPKs, PI3K/Akt, and GSK-3β to 364.80 ± 41.19%, 162.70 ± 5.66%, 265.00 ± 21.06%, 114.00 ± 5.88%, and 97.71 ± 3.06% of the control values, respectively ($p < 0.01$ and $p < 0.001$).

Effects of EUE on LPS-induced phosphorylation of IκBα, degradation of IκBα, and activation of NF-κB in BV-2 microglial cells

The pro-inflammatory response and cytokine production are tightly regulated by multiple signaling molecules, such as IκBα. We thus evaluated the cytoplasmic levels of IκBα after LPS stimulation and EUE-mediated inhibition by Western blotting. Treatment with LPS significantly decreased degradation of IκBα to 32.57 ± 9.43% of the control value (Fig. 6A, $p < 0.001$), whereas phosphorylation of IκBα was significantly increased to 356.80 ± 38.93% of the control value (Fig. 6B, $p < 0.001$). However, this decreased degradation of IκBα was significantly inhibited by 25, 50, and 100 μg/ml EUE to 56.42 ± 6.55%, 70.57 ± 2.65%, and 78.52 ± 2.39% of the control value, respectively ($p < 0.05$, $p < 0.01$, and $p < 0.001$). In addition, pretreatment with 25, 50, and 100 µg/ml EUE significantly inhibited phosphorylation of IκBα to 250.50 ± 24.71%, 150.20 ± 8.01%, and 126.10 ± 19.49% of the control value, respectively ($p < 0.01$ and $p < 0.001$). Next, we investigated whether EUE inhibits the nuclear translocation of NF-κB by Western blotting and immunocytochemistry. Treatment with LPS significantly induced NF-κB translocation from the cytoplasm to the nucleus, as reflected by the increased levels of nuclear NF-κB, to
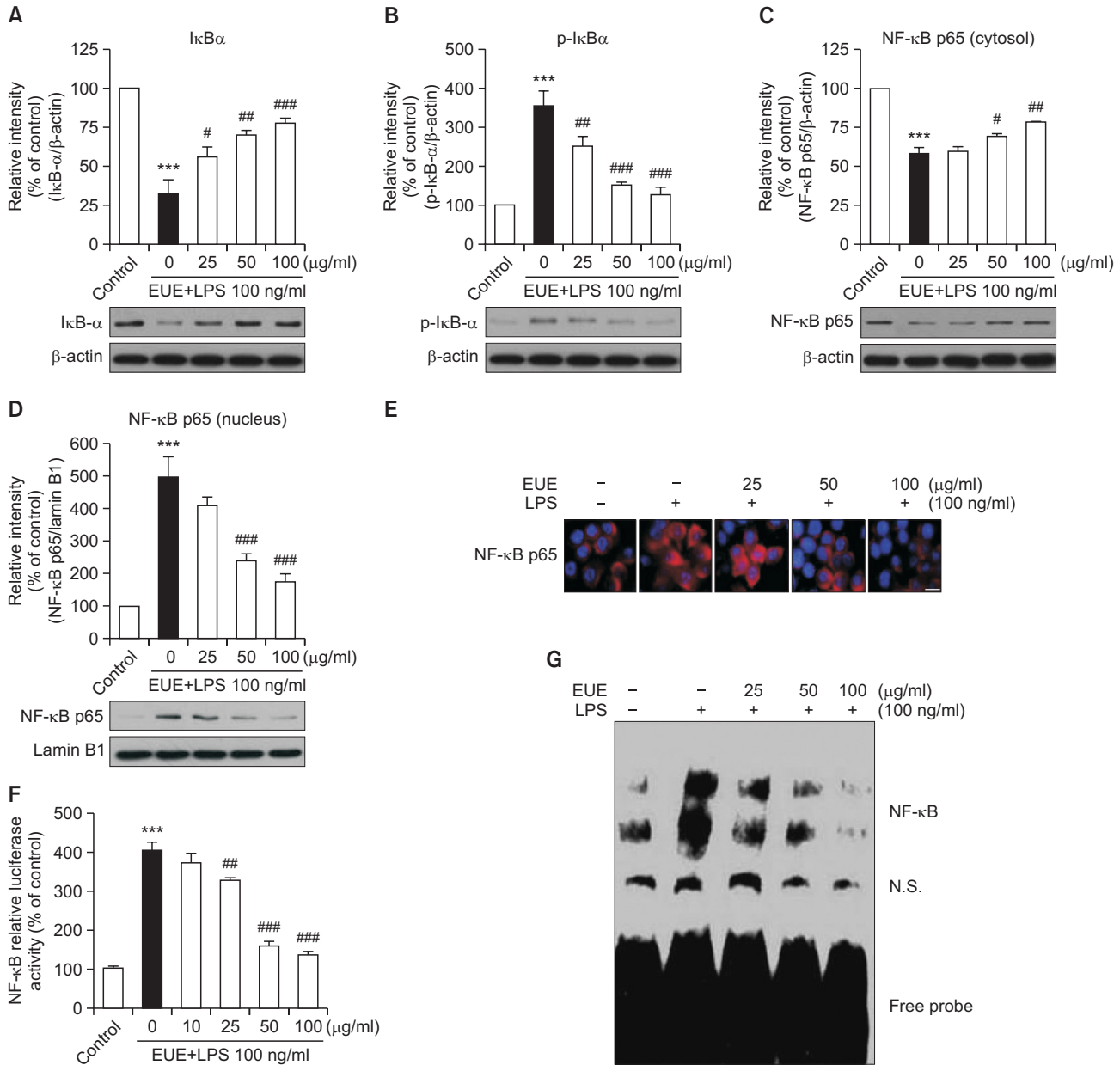
Fig. 6. Effects of EUE on LPS-induced phosphorylation of IκBα (A), degradation of IκBα (B), and activation of NF-κB in BV-2 microglial cells. Cells were pretreated with the indicated concentrations of EUE for 30 min and then stimulated with 100 ng/ml LPS for 1 h. The levels of IκBα, NF-κB p65, β-actin, and lamin B1 were measured by Western blot analysis (A-D). Densitometric results are presented as means ± S.E.M. (n=3). (E) Immunofluorescence analysis of NF-κB p65. Cells were immunostained with anti-NF-κB p65 antibodies and Texas Red®-conjugated secondary antibodies. Nuclei were counterstained with Hoechst 33258, and representative pictures were taken with a fluorescence microscope (100x magnification). Images shown are representative of three independent experiments. Scale bar: 200 μm. (F) Cells were transiently transfected with an NF-κB reporter construct, pretreated with the indicated concentrations of EUE for 30 min, and then stimulated with 100 ng/ml LPS for 1 h. Equal protein amounts of cell extracts were assayed for dual-luciferase activity. Data are presented as means ± S.E.M. (n=3). (G) Cells were pretreated with the indicated concentrations of EUE for 30 min and then stimulated with 100 ng/ml LPS for 1 h. The DNA binding of NF-κB in nuclear extracts was then assayed by EMSAs. ***$p < 0.001$ compared with the control group. #$p < 0.05$; ##$p < 0.01$; and ###$p < 0.001$ compared with the LPStreated group.

58.55 ± 3.94% and 497.50 ± 61.03% of the control values, respectively (Fig. 6B, 6C, $p < 0.001$). However, LPS-induced NF-κB translocation was significantly inhibited by 50 μg/ml EUE to 69.63 ± 1.44% and 239.20 ± 21.83% of the control values, respectively ($p < 0.05$ and $p < 0.001$). Pretreatment with 100 μg/ml EUE also significantly inhibited NF-κB translocation to 78.43 ±

0.32% and 175.40 ± 23.98% of the control values, respectively ($p < 0.01$ and $p < 0.001$). The intracellular localization of NF-κB was clearly visible by immunocytochemical analysis of LPS-treated cells (Fig. 6E). As expected, treatment with EUE significantly blocked LPS-mediated nuclear translocation of NF-κB in BV-2 microglial cells.
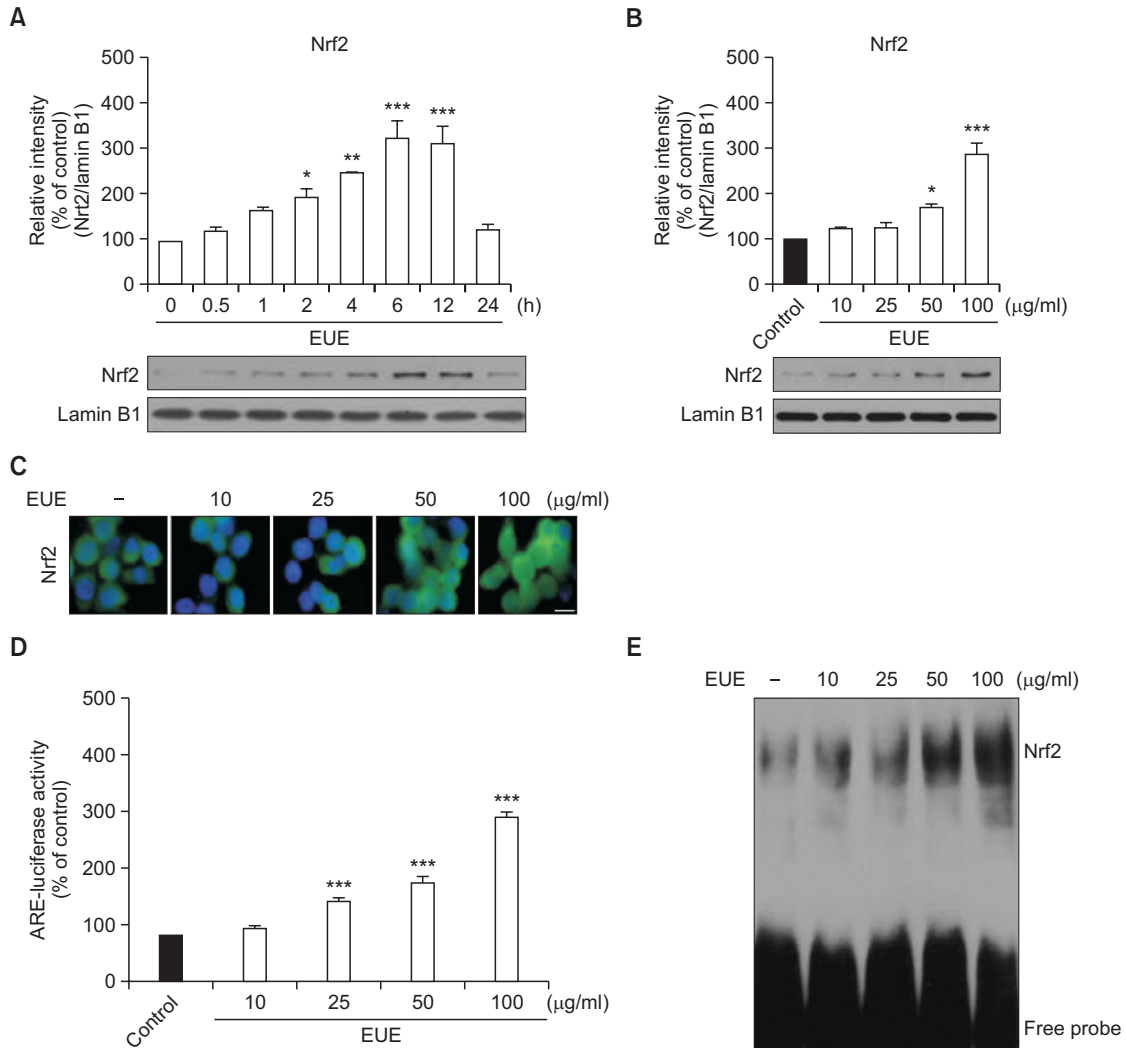
Fig. 7. EUE induces nuclear translocation of Nrf2 in BV-2 microglial cells. (A) Time-dependent EUEmediated induction of Nrf2 nuclear translocation. Cells were treated with 100 μg/ml EUE for 0.5, 1, 2, 4, 6, 12, and 24 h. Nuclear fractions were then prepared and assayed for the presence of Nrf2. (B) Concentrationdependent induction of nuclear translocation of Nrf2 by EUE. Cells were treated with different concentrations of EUE for 6 h. Nuclear fractions were then prepared and analyzed for the presence of Nrf2 and lamin B1 by Western blotting. Densitometric results are presented as means ± S.E.M. (n=3). (C) Immunofluorescence analysis of Nrf2 nuclear translocation. Nrf2 was detected with anti-Nrf2 antibodies and Alexa Fluor® 488-conjugated secondary antibodies. Nuclei were counterstained with Hoechst 33258, and representative pictures were captured with a fluorescence microscope (100× magnification). The images shown are representative of three experiments. Scale bar: 200 μm. (D) ARE reporter assay with EUE. Cells were transiently transfected with an ARE reporter construct and then treated with the indicated concentrations of EUE for 6 h. Equal protein amounts of cell extracts were then assayed for dual-luciferase activity. Data are presented as means ± S.E.M. (n=3). (E) EMSA analysis of DNA binding by Nrf2. Cells were pretreated with the indicated concentrations of EUE for 6 h and nuclear extracts were then prepared. The binding of Nrf2 to DNA was investigated by EMSAs. *$p<0.05$; **$p<0.01$; and ***$p<0.001$ compared with the control group.

Given the inhibitory effects of EUE on LPS-induced nuclear translocation of NF-κB, we measured NF-κB-driven transcription using a luciferase reporter assay. In this assay, BV-2 microglial cells were transfected with an NF-κB reporter construct and its activity was assessed after various treatments. As shown in Fig. 6F, treatment with LPS significantly increased NF-κB activation to 405.30 ± 18.61% of the control value ($p<0.001$). Moreover, NF-κB activation was significantly inhibited by 25, 50, and 100 μg/ml EUE to 328.70 ± 4.93%, 159.10 ± 13.81%, and 138.10 ± 7.25% of the control value, respectively ($p<0.01$ and $p<0.001$). Since NF-κB is a DNA-binding transcription factor, we examined whether EUE

modulates LPS-induced binding of NF-κB to DNA in BV-2 microglial cells. Treatment with LPS significantly increased the binding of NF-κB to DNA, as assessed by EMSA (Fig. 6G). In contrast, pretreatment with EUE significantly suppressed this LPS-induced increase of NF-κB DNA binding.

EUE induces nuclear translocation of Nrf2 in BV-2 microglial cells

We next examined the effects of EUE on HO-1 expression, which is directly linked to Nrf2-dependent activation. As shown in Fig. 7A, 7B, treatment with EUE significantly induced the nuclear translocation of Nrf2 in a time-dependent (Fig. 7A)
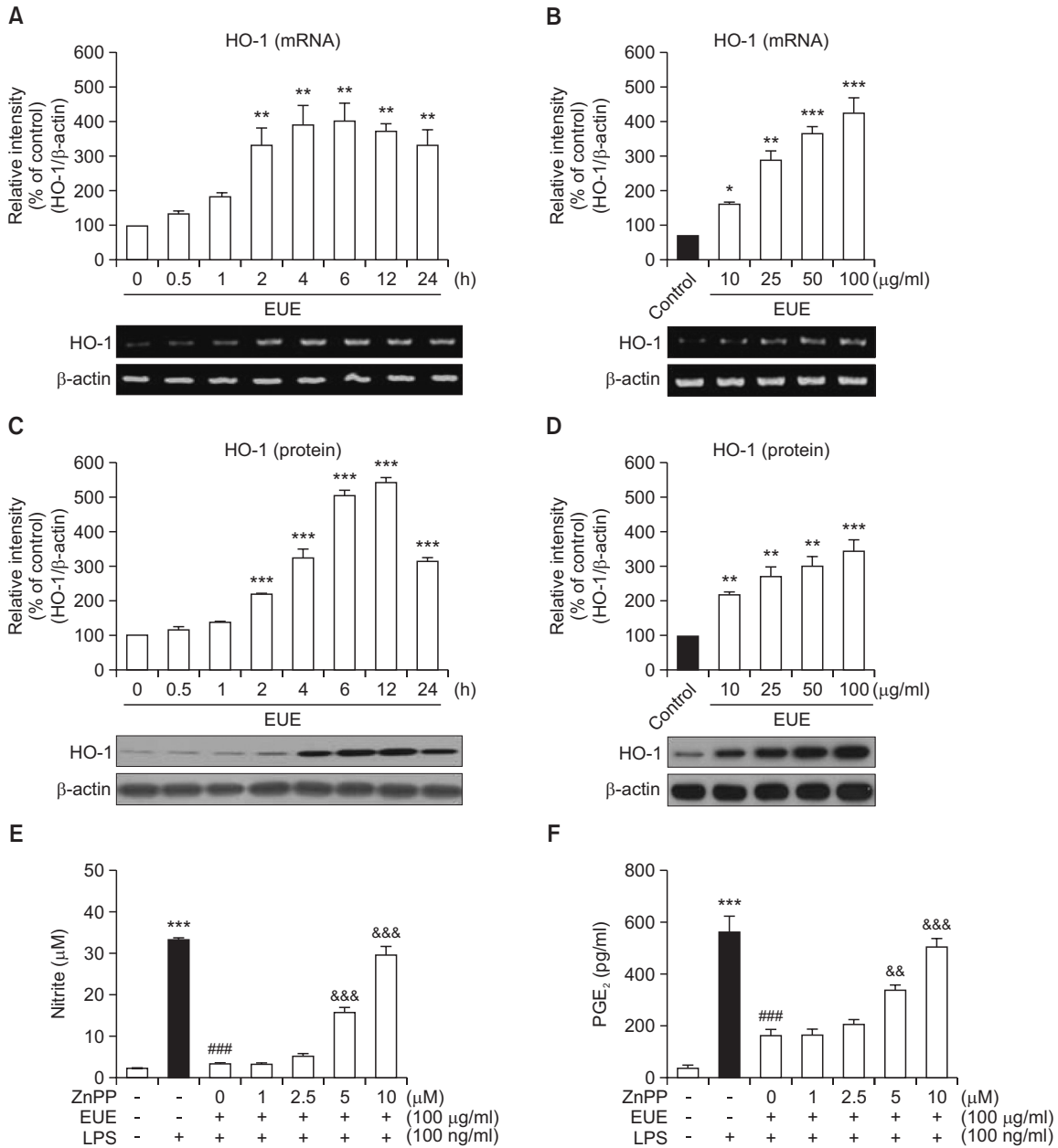
Fig. 8. EUE drives Nrf2-dependent induction of HO-1 in BV-2 microglial cells. (A and C) EUE induces HO-1 expression in a time-dependent manner. Cells were treated with 100 μg/ml EUE for 0.5, 1, 2, 4, 6, 12, and 24 h. The protein and mRNA levels of HO-1 were measured by Western blot and RT-PCR analysis, respectively. (B and D) EUE induces HO-1 expression in a concentration-dependent manner. Cells were treated with the indicated concentrations of EUE for 6 or 12 h, and the protein and mRNA levels of HO-1 were determined by Western blot and RT-PCR analysis, respectively. (B) Western blot analysis of the expression levels of Nrf2, HO-1, β-actin, and GAPDH. Densitometric results are presented as means ± S.E.M. (n=3). (D) RT-PCR analysis of the mRNA levels of HO-1 and β-actin. Expression results are presented as means ± S.E.M. (n=3). *$p<0.05$; **$p<0.01$; and ***$p<0.001$ compared with the control group. (E and F) Treatment with ZnPP prevents EUE-mediated inhibition of LPS-stimulated production of NO (E) and PGE2 (F). Cells were pretreated with the indicated concentrations of ZnPP for 1 h, incubated with 100 μg/ml EUE for 30 min, and then stimulated with 100 ng/ml LPS for 24 h. The concentrations of nitrite in the culture medium were then determined using the Griess reagent. Data are presented as means ± S.E.M. (n=6). ***$p<0.001$ compared with the control group. ###$p<0.001$ compared with the LPS-treated group. &&$p<0.01$ and &&&$p<0.001$ compared with the EUE+LPS-treated group.

and concentration-dependent (Fig. 7B) manner. The levels of nuclear Nrf2 were significantly increased 2 h after treatment with 100 μg/ml EUE, peaked at 6 h, and then decreased at 12 h. Thus, treatment with 100 μg/ml EUE for 6 h was used to induce the nuclear translocation of Nrf2 in all subsequent

experiments. Immunocytochemical analysis clearly revealed Nrf2 accumulation in the nuclei of EUE-treated BV-2 microglial cells (Fig. 7C). To investigate whether ARE binding by Nrf2 plays a role in EUE-mediated induction of HO-1 expression, cells were transfected with luciferase reporters under

the control of the ARE promoter. As shown in Fig. 7D, EUE potently induced ARE-mediated transcription of luciferase in BV-2 microglial cells transfected with the ARE reporter construct. Moreover, ARE-driven transcription was significantly increased by treatment with 25, 50, and 100 μg/ml EUE to 176.70 ± 4.44%, 214.80 ± 12.85%, and 359.30 ± 11.64% of the control value, respectively ($p<0.001$). To directly test whether EUE activates Nrf2, EMSAs were performed to examine the binding of Nrf2 to DNA in nuclear extracts prepared from EUE-treated BV-2 microglial cells. These experiments showed that EUE significantly increased Nrf2 binding to DNA in a concentration-dependent manner (Fig. 7E).

EUE stimulates Nrf2-mediated induction of HO-1 in BV-2 microglial cells

To determine whether the observed anti-neuroinflammatory effects of EUE were accompanied by activation of the Nrf2-ARE pathway in BV-2 microglial cells, we analyzed the protein and mRNA levels of HO-1, a downstream target of Nrf2, by Western blotting and RT-PCR. Treatment with EUE resulted in a time-dependent (Fig. 8A, 8C) and concentration-dependent (Fig. 8B, 8D) increase in the levels of HO-1 protein and mRNA. Both the mRNA and protein levels of HO-1 were significantly increased at 2 h after treatment with 100 μg/ml EUE and peaked at 6 h and 12 h, respectively. We next investigated whether HO-1 is the downstream target of Nrf2 that mediates the anti-inflammatory activity of EUE against LPS-stimulated inflammatory responses in BV-2 microglial cells. To this end, we tested the effects of ZnPP, an HO-1-specific inhibitor, on the anti-inflammatory effects of EUE. As shown in Fig. 8E and 8F, treatment with LPS significantly increased the levels of secreted NO and PGE$_2$ by 33.42 ± 0.48 μM and 564.60 ± 59.07 pg/ml more than the control values, respectively ($p<0.001$). This increased NO and PGE$_2$ production was significantly inhibited by treatment with 100 μg/ml EUE, to 3.56 ± 0.26 μM and 164.00 ± 24.91 pg/ml greater than the control values, respectively ($p<0.001$). However, EUE-mediated inhibition of NO production was markedly blocked by pretreatment with ZnPP at 5 or 10 μM, such that the levels of secreted NO were only 15.95 ± 1.23 μM and 29.60 ± 1.53 μM above the control values, respectively ($p<0.001$). Similarly, EUE-mediated inhibition of PGE$_2$ production was significantly prevented by pretreatment with 5 or 10 μM ZnPP. Specifically, the levels of PGE$_2$ were 337.30 ± 23.67 μM and 506.50 ± 31.85 μM above the control values, respectively ($p<0.01$ and $p<0.001$).

DISCUSSION

The main finding of this study is that EUE potently inhibits pro-inflammatory responses in microglia, most likely by inhibiting NF-κB activation and thus preventing Nrf2-mediated up-regulation of HO-1 expression. To the best of our knowledge, this is the first report to demonstrate that NF-κB activation and Nrf2-dependent HO-1 expression mediate the anti-neuroinflammatory effects of EUE. It is also the first report to identify the molecular mechanisms by which EUE modulates pro-inflammatory molecule production in BV-2 microglial cells.

NO and PGE$_2$ are important mediators of inflammation. These two molecules are thought to be responsible for some of the damage that is seen in the CNS in brain injuries and diseases such as AD, PD, and stroke.(Minghetti and Levi,

1998) NO is synthesized from L-arginine by NO synthase, which is comprised of three enzymes. One of these enzymes is iNOS, which is produced mainly by activated glial cells (Lee et al., 2003). Thus, inhibition of iNOS and NO synthase is one possible approach for preventing the development of inflammatory diseases. PGE$_2$ is another well-characterized inflammatory mediator that is derived from arachidonic acid via the action of cyclooxygenases. Overproduction of PGE$_2$ in response to growth factors, cytokines, and pro-inflammatory molecules is associated with upregulation of COX-2 (Minghetti et al., 1999). Both iNOS and COX-2 have been reported to be induced in various types of CNS injuries and diseases (Minghetti, 2004). These enzymes are believed to contribute to the pathogenesis of AD, PD, and stroke, as assessed by postmortem examinations of various patients (Lucas et al., 2006; Heneka and O'Banion, 2007; Amor et al., 2010). In addition, iNOS and COX-2 have been shown to be upregulated in microglial cells in rodent brains after LPS treatment (Boje and Arora, 1992). Thus, compounds that inhibit the expression of iNOS and COX-2 may be able to prevent and/or delay the progression of neurodegenerative diseases. In the present study, we initially determined whether EUE inhibits the production of NO and PGE$_2$. We also investigated whether EUE-mediated inhibition involved the downregulation of iNOS and COX-2 expression at the mRNA and protein levels. We found that EUE significantly inhibited the production of both NO and PGE$_2$ in a concentration-dependent manner, and that these inhibitory effects were mediated by the downregulation of COX-2 and iNOS expression on both the mRNA and protein levels. These results indicate that EUE may be beneficial in treating microglial inflammation, since EUE is able to inhibit the initial stages of inflammation.

Pro-inflammatory cytokines such as TNF-α and IL-1β have been shown to promote neuronal injury by activated microglia (Block et al., 2007). TNF-α is a key downstream mediator in pro-inflammatory responses, and has various pro-inflammatory effects on many different cell types. Microglia are major producers of TNF-α in the brain and may play a role in certain pathological conditions in the brain (Rock et al., 2004). TNF-α overexpression has been implicated in the pathogenesis of several human CNS disorders such as AD, PD, and stroke (Botchkina et al., 1997; Mattson and Camandola, 2001; Sriram et al., 2002). IL-1β is another potent pro-inflammatory cytokine that acts through IL-1 receptors expressed by numerous cell types, including neurons and microglia. Moreover, IL-1β has been proposed to be an important mediator of neuroimmune interactions that participate directly in neurodegeneration (Rothwell et al., 1997). Consequently, the inhibition of cytokine production and/or function is a key mechanism by which CNS inflammation is controlled. Thus, we assessed whether EUE could inhibit the production of LPS-induced pro-inflammatory cytokines, including TNF-α and IL-1β, in BV-2 microglial cells. We found that EUE significantly inhibited LPS-mediated upregulation of mRNA expression and production of two pro-inflammatory cytokines, TNF-α and IL-1β, in BV-2 microglial cells. Consistent with our results, EUE has been shown to inhibit TNF-α and IL-6 production in LPS-stimulated murine peritoneal macrophage cells (Kim et al., 2012). This result indicates that EUE is able to modulate the activities of TNF-α and IL-1β on either the transcriptional or protein level in activated microglia.

Elevated ROS levels have been found to be associated

with neurodegenerative diseases such as AD, PD, and stroke (Block *et al*., 2007). Recent studies have demonstrated that activated microglia are important sources of ROS in the brain and are involved in neuro-inflammatory processes in neuro-degenerative diseases (Amor *et al*., 2010). Overproduction of ROS in microglial cells is strongly linked to brain injuries with high levels of pro-inflammatory mediators and/or cyto-kines (Floyd and Hensley, 2002). Moreover, ROS can trigger a cascade of deleterious events in the inflammatory process via MAPKs, PI3K/Akt, and GSK-3β. Signaling through these mol-ecules leads to the activation of NF-κB and the subsequent overexpression of neuro-inflammatory molecules in activated microglial cells (Salminen *et al*., 2008; Hsieh *et al*., 2010; Kois-tinaho *et al*., 2011). Thus, suppression of ROS production may be an effective way by which microglial cells can be protected from inflammatory damage. To evaluate whether the inhibitory effects of EUE on ROS accumulation involve the activation of MAPKs, PI3K/Akt, GSK-3β, or NF-κB, we examined ROS production in BV-2 microglial cells. We found that EUE sig-nificantly inhibited LPS-induced intracellular ROS production in BV-2 microglial cells, suggesting a possible mechanism by which EUE inhibits the activation of NF-κB, MAPKs, PI3K/Akt, and GSK-3β. This finding is in agreement with our previous observation that EUE is an effective neuroprotective agent against oxidative stress (H_2O_2)-mediated death in neuronal SH-SY5Y cells (Kwon *et al*., 2012). Furthermore, EUE-medi-ated inhibition of ROS production might prevent the produc-tion of pro-inflammatory mediators and/or cytokines, thereby reducing inflammation.

Various intracellular signaling pathways are involved in me-diating the inflammatory response. Many signaling proteins such as MAPKs, PI3K/Akt, and GSK-3β are phosphorylated in response to LPS treatment. These proteins regulate the pro-inflammatory response and cytokine production in microglial cells (Kaminska, 2005; Wang *et al*., 2007; Smith *et al*., 2012). Previous studies have shown that activation of MAPKs, PI3K/Akt, and GSK-3β has a significant effect on iNOS, COX-2, and pro-inflammatory cytokine gene expression in microglia by controlling the activation of NF-κB (Surh *et al*., 2001; Li *et al*., 2006; Yuskaitis and Jope, 2009). Thus, MAPKs, PI3K/Akt, and GSK-3β are essential mediators of pro-inflammatory mol-ecules in microglia, and interventions in these pathways may be valid therapeutic approaches for treating inflammation-re-lated neurological diseases. Although the effects of EUE on oxidative stress-induced activation of the MAPK and PI3K/Akt signaling pathways have been described (Kwon *et al*., 2012), the mechanisms underlying the interactions of EUE with these signaling pathways are not yet fully understood. In particular, it was unknown whether EUE exerts its anti-inflammatory ef-fects by regulating MAPK, PI3K/Akt, and GSK-3β in activated microglia. Therefore, in this study we determined whether EUE regulates the activation of MAPKs, PI3K/Akt, and GSK-3β in LPS-activated BV-2 microglial cells. We found that EUE po-tently inhibits the phosphorylation of MAPKs, PI3K/Akt, and GSK-3β. These findings suggest that EUE suppresses key sig-nal transduction pathways that are normally activated by LPS in BV-2 microglial cells, thereby preventing LPS-mediated upreg-ulation of iNOS and COX-2 expression and NF-κB activation.

Activation of NF-κB in microglia contributes to neuronal injury and promotes the development of neurodegenerative diseases such as AD, PD, and stroke (Mattson, 2005). NF-κB is also a central regulator of microglial responses to various stimuli such as LPS and cytokines (O'Neill and Kaltschmidt, 1997). The mechanism by which NF-κB acts is well character-ized: NF-κB is normally inactive when bound to IκBα in the cytoplasm in microglial cells. However, in response to stress, phosphorylated IκBα is degraded through selective ubiquitina-tion, resulting in the activation of NF-κB. Activated NF-κB then translocates to the nucleus and binds to the promoter regions of pro-inflammatory genes, thereby upregulating the expres-sion of these molecules (Nomura, 2001). Therefore, inhibition of these signaling pathways may explain the potent EUE-me-diated suppression of the inflammatory response observed in the present study. We found that EUE inhibited LPS-induced phosphorylation of IκBα, degradation of IκBα, and nuclear translocation of NF-κB in BV-2 microglial cells. Furthermore, EUE also significantly repressed DNA binding by NF-κB and NF-κB-driven transcription upon LPS-mediated activation of microglial cells. These findings suggest that EUE-mediated down-regulation of inflammatory mediators results from the inhibition of NF-κB signaling pathways, ultimately resulting in anti-neuro-inflammatory effects.

Nrf2 is expressed in most cell types of the brain, including microglia. Activation of Nrf2 in microglia following brain injury is known to play a role in inhibiting microglial hyperactivation and in preventing neuronal death caused by microgliosis. Moreover, recent studies have reported that ROS are gener-ated in response to inflammatory signals and participate in microglial activation (Fremond *et al*., 2007); moreover, Nrf2 has been shown to modulate brain redox homeostasis and regulate inflammation (Lee *et al*., 2011). Therefore, Nrf2 sig-naling may be an attractive therapeutic target for the treatment of neurodegenerative diseases (Innamorato *et al*., 2008). We hypothesized that the anti-inflammatory actions of EUE were mediated by the Nrf2 signaling pathway. To test this hypoth-esis, we examined the effects of EUE on the nuclear translo-cation of Nrf2 and on the binding of Nrf2 to AREs. We found that EUE significantly induced Nrf2 nuclear translocation and stimulated Nrf2 binding to AREs in microglial cells, demon-strating activation of the anti-inflammatory response pathway. These findings suggest that induction of HO-1 expression by EUE involves Nrf2-mediated transcription at AREs.

HO-1 is an enzyme with potent anti-inflammatory and anti-oxidant effects. A large body of evidence suggests that HO-1 plays a key role in maintaining anti-oxidant homeostasis dur-ing cellular stress (Maines, 1988). The induction of HO-1 ex-pression is primarily regulated at the transcriptional level by various transcription factors and is also linked to Nrf2. In the light of growing evidence indicating that HO-1 provides neu-roprotection, elevating HO-1 expression by a pharmacologic modulator may represent a valid strategy for therapeutic in-tervention. In particular, the identification of a non-cytotoxic inducer of HO-1 expression could enhance the anti-oxidant potential of cells. Therefore, since HO-1 is an important component of cellular defenses against the inflammatory re-sponse, we assessed whether EUE could induce HO-1 ex-pression to strengthen the anti-inflammatory response. We found that EUE upregulates HO-1 expression via Nrf2-medi-ated ARE activation. Moreover, many studies have suggested that HO-1 plays a pivotal protective role in inflammatory re-sponses due to its ability to inhibit pro-inflammatory responses such as NO production (Takagi *et al*., 2010). This observation suggests that HO-1 is a potential therapeutic target for treating inflammatory neurodegenerative diseases (Kang *et al*., 2013).

In this study, we found that EUE significantly increased the expression of HO-1. ZnPP, a specific inhibitor of HO-1, significantly prevented EUE-mediated inhibition of NO production in LPS-stimulated BV-2 microglial cells. Taken together, these data support a model in which EUE induces HO-1 expression in BV-2 microglial cells, thereby conferring neuroprotection against pro-inflammatory responses. EUE induces Nrf2 nuclear translocation, which is upstream of EUE-mediated induction of HO-1 expression. In addition, HO-1 is a main effector molecule in LPS-induced NO and PGE_2 production, and EUE-mediated inhibition of NO and PGE_2 production is partially regulated by HO-1 expression. Therefore, our data support a model in which expression of HO-1, a key phase II detoxifying enzyme, mediates the anti-inflammatory effects of EUE via Nrf2 signaling pathways.

Considering the current literature and the data reported here, inhibition of pro-inflammatory responses mediated by EUE appears to be associated with suppression of NF-κB and activation of HO-1/Nrf2, which are signaling molecules involved in neuro-inflammation. The primary compounds from EUE reported to be responsible for various pharmacological actions, particularly chlorogenic acid (CGA), were also evaluated previously for neuroprotective effects against oxidative stress-induced cell death in neuronal cells (Kwon *et al*., 2014). Recently, CGA inhibits the inflammatory reaction in herpes simplex virus encephalitis via the suppression of Toll-like receptors/myeloid differentiation factor88 signaling pathways in BV-2 microglial cells (Guo *et al*., 2015). CGA may serves as an anti-inflammatory agent and provide a new strategy for treating neuro-inflammation-related diseases. However, further studies are needed to elucidate the precise anti-inflammatory activities of standardized EUE's compounds *in vivo* and/or *in vitro* systems. We are currently working to isolate EUE's active components using an activity-guided fractionation approach.

In summary, the present study showed the potential anti-inflammatory effects of EUE in BV-2 microglial cells. In LPS-stimulated BV-2 microglial cells, EUE significantly inhibited the production of two inflammatory mediators, NO and PGE_2, and suppressed the expression and release of multiple molecules involved in inflammation, including iNOS, COX-2, TNF-α, and IL-1β. EUE also significantly attenuated intracellular ROS accumulation in LPS-stimulated BV-2 microglial cells. These inhibitory effects of EUE were associated with reduced phosphorylation of MAPKs, PI3K/Akt, and GSK-3β. They were also associated with reduced activation of NF-κB. In addition, EUE induces HO-1 expression in BV-2 microglial cells, which confers protection against the LPS-induced inflammatory response. EUE also induces Nrf2 nuclear translocation, which occurs upstream of EUE-induced HO-1 expression. Although we did not evaluate whether EUE protects against inflammation-related neuronal damage *in vivo*, we did demonstrate that EUE exerts anti-inflammatory activities in BV-2 microglial cells. The regulation of inflammatory molecules by EUE may have therapeutic potential in the treatment of various neurodegenerative diseases. Accordingly, our findings suggest that EUE could be used as a therapeutic agent in the treatment of neuro-inflammation-associated disorders.

CONFLICTS OF INTEREST

The authors have no conflicts of interest to declare.

REFERENCES

Amor, S., Puentes, F., Baker, D. and van der Valk, P. (2010) Inflammation in neurodegenerative diseases. *Immunology* **129**, 154-169.

Baima, E. T., Guzova, J. A., Mathialagan, S., Nagiec, E. E., Hardy, M. M., Song, L. R., Bonar, S. L., Weinberg, R. A., Selness, S. R., Woodard, S. S., Chrencik, J., Hood, W. F., Schindler, J. F., Kishore, N. and Mbalaviele, G. (2010) Novel insights into the cellular mechanisms of the anti-inflammatory effects of NF-κB essential modulator binding domain peptides. *J. Biol. Chem.* **285**, 13498-13506.

Bauer, M. and Bauer, I. (2002) Heme oxygenase-1: redox regulation and role in the hepatic response to oxidative stress. *Antioxid. Redox Signal.* **4**, 749-758.

Block, M. L. and Hong, J. S. (2005) Microglia and inflammation-mediated neurodegeneration: multiple triggers with a common mechanism. *Prog. Neurobiol.* **76**, 77-98.

Block, M. L., Zecca, L. and Hong, J. S. (2007) Microglia-mediated neurotoxicity: uncovering the molecular mechanisms. *Nat. Rev. Neurosci.* **8**, 57-69.

Boje, K. M. and Arora, P. K. (1992) Microglial-produced nitric oxide and reactive nitrogen oxides mediate neuronal cell death. *Brain Res.* **587**, 250-256.

Botchkina, G. I., Meistrell, M. E., 3rd, Botchkina, I. L. and Tracey, K. J. (1997) Expression of TNF and TNF receptors (p55 and p75) in the rat brain after focal cerebral ischemia. *Mol. Med.* **3**, 765-781.

Floyd, R. A. and Hensley, K. (2002) Oxidative stress in brain aging. Implications for therapeutics of neurodegenerative diseases. *Neurobiol. Aging* **23**, 795-807.

Fremond, C. M., Togbe, D., Doz, E., Rose, S., Vasseur, V., Maillet, I., Jacobs, M., Ryffel, B. and Quesniaux, V. F. (2007) IL-1 receptor-mediated signal is an essential component of MyD88-dependent innate response to Mycobacterium tuberculosis infection. *J. Immunol.* **179**, 1178-1189.

Gao, H. M. and Hong, J. S. (2008) Why neurodegenerative diseases are progressive: uncontrolled inflammation drives disease progression. *Trends Immunol.* **29**, 357-365.

Guo, Y. J., Luo, T., Wu, F., Mei, Y. W., Peng J., Liu, H., Li, H. R., Zhang, S. L., Dong, J. H., Fang, Y., Zhao, L. (2015) Involvement of TLR2 and TLR9 in the anti-inflammatory effects of chlorogenic acid in HSV-1-infected microglia. *Life Sci.* **127**, 12-18.

Heneka, M. T. and O'Banion, M. K. (2007) Inflammatory processes in Alzheimer's disease. *J. Neuroimmunol.* **184**, 69-91.

Hsieh, H. L., Wang, H. H., Wu, W. B., Chu, P. J. and Yang, C. M. (2010) Transforming growth factor-β1 induces matrix metalloproteinase-9 and cell migration in astrocytes: roles of ROS-dependent ERK- and JNK-NF-κB pathways. *J. Neuroinflammation* **7**, 88.

Innamorato, N. G., Rojo, A. I., García-Yagüe, A. J., Yamamoto, M., de Ceballos, M. L. and Cuadrado, A. (2008) The transcription factor Nrf2 is a therapeutic target against brain inflammation. *J. Immunol.* **181**, 680-689.

Jiang, L., Wang, Z., Zhu, H. W., Di, H. Y., Li, H., Zhang, Y. Y. and Chen, D. F. (2011) Beneficial effect of *Eucommia* polysaccharides on systemic lupus erythematosus-like syndrome induced by Campylobacter jejuni in BALB/c mice. *Inflammation* **34**, 402-411.

Kaminska, B. (2005) MAPK signalling pathways as molecular targets for anti-inflammatory therapy--from molecular mechanisms to therapeutic benefits. *Biochim. Biophys. Acta* **1754**, 253-262.

Kang, C. H., Kim, M. J., Seo, M. J., Choi, Y. H., Jo, W. S., Lee, K. T., Jeong, Y. K. and Kim, G. Y. (2013) 5-Hydroxy-3,6,7,8,3'4'-hexamethoxyflavone inhibits nitric oxide production in lipopolysaccharide-stimulated BV2 microglia via NF-κB suppression and Nrf-2-de-

pendent heme oxygenase-1 induction. *Food Chem. Toxicol.* **57**, 119-125.

Kensler, T. W., Wakabayashi, N. and Biswal, S. (2007) Cell survival responses to environmental stresses via the Keap1-Nrf2-ARE pathway. *Annu. Rev. Pharmacol. Toxicol.* **47**, 89-116.

Kim, B. H., Park, K. S. and Chang, I. M. (2009) Elucidation of anti-inflammatory potencies of *Eucommia ulmoides* bark and Plantago asiatica seeds. *J. Med. Food* **12**, 764-769.

Kim, J., Cha, Y. N. and Surh, Y. J. (2010) A protective role of nuclear factor-erythroid 2-related factor-2 (Nrf2) in inflammatory disorders. *Mutat. Res.* **690**, 12-23.

Kim, M. C., Kim, D. S., Kim, S. J., Park, J., Kim, H. L., Kim, S. Y., Ahn, K. S., Jang, H. J., Lee, S. G., Lee, K. M., Hong, S. H. and Um, J. Y. (2012) *Eucommiae* cortex inhibits TNF-α and IL-6 through the suppression of caspase-1 in lipopolysaccharide-stimulated mouse peritoneal macrophages. *Am. J. Chin. Med.* **40**, 135-149.

Koistinaho, J., Malm, T. and Goldsteins, G. (2011) Glycogen synthase kinase-3β: a mediator of inflammation in Alzheimer's disease? *Int. J. Alzheimers Dis.* **2011**, 129753.

Krönke, G., Bochkov, V. N., Huber, J., Gruber, F., Blüml, S., Fürnkranz, A., Kadl, A., Binder, B. R. and Leitinger, N. (2003) Oxidized phospholipids induce expression of human heme oxygenase-1 involving activation of cAMP-responsive element-binding protein. *J. Biol. Chem.* **278**, 51006-51014.

Kwan, C. Y., Chen, C. X., Deyama, T. and Nishibe, S. (2003) Endothelium-dependent vasorelaxant effects of the aqueous extracts of the *Eucommia ulmoides* Oliv. leaf and bark: implications on their antihypertensive action. *Vascul. Pharmacol.* **40**, 229-235.

Kwon, S. H., Ma, S. X., Hong, S. I., Kim, S. Y., Lee, S. Y. and Jang, C. G. (2014) *Eucommia ulmoides* Oliv. bark. attenuates 6-hydroxydopamine-induced neuronal cell death through inhibition of oxidative stress in SH-SY5Y cells. *J. Ethnopharmacol.* **152**, 173-182.

Kwon, S. H., Kim, M. J., Ma, S. X., You, I. J., Hwang, J. Y., Oh, J. H., Kim, S. Y., Kim, H. C., Lee, S. Y. and Jang, C. G. (2012) *Eucommia ulmoides* Oliv. Bark. protects against hydrogen peroxide-induced neuronal cell death in SH-SY5Y cells. *J. Ethnopharmacol.* **142**, 337-345.

Kwon, S. H., Lee, H. K., Kim, J. A., Hong, S. I., Kim, S. Y., Jo, T. H., Park, Y. I., Lee, C. K., Kim, Y. B., Lee, S. Y. and Jang, C. G. (2011) Neuroprotective effects of *Eucommia ulmoides* Oliv. Bark on amyloid beta$_{25-35}$-induced learning and memory impairments in mice. *Neurosci. Lett.* **487**, 123-127.

Lee, I. S., Lim, J., Gal, J., Kang, J. C., Kim, H. J., Kang, B. Y. and Choi, H. J. (2011) Anti-inflammatory activity of xanthohumol involves heme oxygenase-1 induction via NRF2-ARE signaling in microglial BV2 cells. *Neurochem. Int.* **58**, 153-160.

Lee, J., Ryu, H., Ferrante, R. J., Morris, S. M., Jr. and Ratan, R. R. (2003) Translational control of inducible nitric oxide synthase expression by arginine can explain the arginine paradox. *Proc. Natl. Acad. Sci. U.S.A.* **100**, 4843-4848.

Lee, M. K., Cho, S. Y., Kim, D. J., Jang, J. Y., Shin, K. H., Park, S. A., Park, E. M., Lee, J. S., Choi, M. S., Lee, J. S. and Kim, M. J. (2005) Du-zhong (*Eucommia ulmoides* Oliv.) cortex water extract alters heme biosynthesis and erythrocyte antioxidant defense system in lead-administered rats. *J. Med. Food* **8**, 86-92.

Li, F., Chong, Z. Z. and Maiese, K. (2006) Microglial integrity is maintained by erythropoietin through integration of Akt and its substrates of glycogen synthase kinase-3β, β-catenin, and nuclear factor-κB. *Curr. Neurovasc. Res.* **3**, 187-201.

Lin, J., Fan, Y. J., Mehl, C., Zhu, J. J., Chen, H., Jin, L. Y., Xu, J. H. and Wang, H. M. (2011) *Eucommia ulmoides* Oliv. antagonizes H_2O_2-induced rat osteoblastic MC3T3-E1 apoptosis by inhibiting expressions of caspases 3, 6, 7, and 9. *J. Zhejiang Univ. Sci. B* **12**, 47-54.

Liu, E., Han, L., Wang, J., He, W., Shang, H., Gao, X. and Wang, T. (2012) *Eucommia ulmoides* bark protects against renal injury in cadmium-challenged rats. *J. Med. Food* **15**, 307-314.

Lucas, S. M., Rothwell, N. J. and Gibson, R. M. (2006) The role of inflammation in CNS injury and disease. *Br. J. Pharmacol.* **147**, S232-S240.

Lull, M. E. and Block, M. L. (2010) Microglial activation and chronic

neurodegeneration. *Neurotherapeutics* **7**, 354-365.

Luo, L. F., Wu, W. H., Zhou, Y. J., Yan, J., Yang, G. P. and Ouyang, D. S. (2010) Antihypertensive effect of *Eucommia ulmoides Oliv.* extracts in spontaneously hypertensive rats. *J. Ethnopharmacol.* **129**, 238-243.

Maines, M. D. (1988) Heme oxygenase: function, multiplicity, regulatory mechanisms, and clinical applications. *FASEB J.* **2**, 2557-2568.

Marchetti, B. and Abbracchio, M. P. (2005) To be or not to be (inflamed)--is that the question in anti-inflammatory drug therapy of neurodegenerative disorders? *Trends Pharmacol. Sci.* **26**, 517-525.

Mattson, M. P. (2005) NF-κB in the survival and plasticity of neurons. *Neurochem. Res.* **30**, 883-893.

Mattson, M. P. and Camandola, S. (2001) NF-κB in neuronal plasticity and neurodegenerative disorders. *J. Clin. Invest.* **107**, 247-254.

Minghetti, L. (2004) Cyclooxygenase-2 (COX-2) in inflammatory and degenerative brain diseases. *J. Neuropathol. Exp. Neurol.* **63**, 901-910.

Minghetti, L. and Levi, G. (1998) Microglia as effector cells in brain damage and repair: focus on prostanoids and nitric oxide. *Prog. Neurobiol.* **54**, 99-125.

Minghetti, L., Walsh, D. T., Levi, G. and Perry, V. H. (1999) *In vivo* expression of cyclooxygenase-2 in rat brain following intraparenchymal injection of bacterial endotoxin and inflammatory cytokines. *J. Neuropathol. Exp. Neurol.* **58**, 1184-1191.

Nomura, Y. (2001) NF-κB activation and IκBα dynamism involved in iNOS and chemokine induction in astroglial cells. *Life Sci.* **68**, 1695-1701.

O'Neill, L. A. and Kaltschmidt, C. (1997) NF-κB: a crucial transcription factor for glial and neuronal cell function. *Trends Neurosci.* **20**, 252-258.

Park, S. Y., Kim, J. H., Lee, S. J. and Kim, Y. (2013) Involvement of PKA and HO-1 signaling in anti-inflammatory effects of surfactin in BV-2 microglial cells. *Toxicol. Appl. Pharmacol.* **268**, 68-78.

Rock, R. B., Gekker, G., Hu, S., Sheng, W. S., Cheeran, M., Lokensgard, J. R. and Peterson, P. K. (2004) Role of microglia in central nervous system infections. *Clin. Microbiol. Rev.* **17**, 942-964.

Rothwell, N., Allan, S. and Toulmond, S. (1997) The role of interleukin 1 in acute neurodegeneration and stroke: pathophysiological and therapeutic implications. *J. Clin. Invest.* **100**, 2648-2652.

Salminen, A., Huuskonen, J., Ojala, J., Kauppinen, A., Kaarniranta, K. and Suuronen, T. (2008) Activation of innate immunity system during aging: NF-kB signaling is the molecular culprit of inflamm-aging. *Ageing Res. Rev.* **7**, 83-105.

Smith, J. A., Das, A., Ray, S. K. and Banik, N. L. (2012) Role of pro-inflammatory cytokines released from microglia in neurodegenerative diseases. *Brain Res. Bull.* **87**, 10-20.

Sriram, K., Matheson, J. M., Benkovic, S. A., Miller, D. B., Luster, M. I. and O'Callaghan, J. P. (2002) Mice deficient in TNF receptors are protected against dopaminergic neurotoxicity: implications for Parkinson's disease. *FASEB J.* **16**, 1474-1476.

Surh, Y. J., Chun, K. S., Cha, H. H., Han, S. S., Keum, Y. S., Park, K. K. and Lee, S. S. (2001) Molecular mechanisms underlying chemopreventive activities of anti-inflammatory phytochemicals: down-regulation of COX-2 and iNOS through suppression of NF-κB activation. *Mutat. Res.* **480-481**, 243-268.

Takagi, T., Naito, Y., Uchiyama, K. and Yoshikawa, T. (2010) The role of heme oxygenase and carbon monoxide in inflammatory bowel disease. *Redox Rep.* **15**, 193-201.

Wang, M. J., Lin, S. Z., Kuo, J. S., Huang, H. Y., Tzeng, S. F., Liao, C. H., Chen, D. C. and Chen, W. F. (2007) Urocortin modulates inflammatory response and neurotoxicity induced by microglial activation. *J. Immunol.* **179**, 6204-6214.

Yang, J., Kato, K., Noguchi, K., Dairaku, N., Koike, T., Iijima, K., Imatani, A., Sekine, H., Ohara, S., Sasano, H. and Shimosegawa, T. (2003) Tochu (*Eucommia ulmoides*) leaf extract prevents ammonia and vitamin C deficiency induced gastric mucosal injury. *Life Sci.* **73**, 3245-3256.

Yuskaitis, C. J. and Jope, R. S. (2009) Glycogen synthase kinase-3 regulates microglial migration, inflammation, and inflammation-induced neurotoxicity. *Cell. Signal.* **21**, 264-273.